International Journal of Modern Physics B
Vol. 28, No. 24 (2014) 1450161 (11 pages)

DOI: 10.1142/S0217979214501616

World Scientific
www.worldscientific.com

Spin and surface orientation effects of work function for Cr/Ni(111), Cr/Ni(100) and Cr/Ni(110) metal gates

Kehua Zhong, Guigui Xu, Yanmin Cheng, Keqin Tang,
Zhigao Chen and Zhigao Huang*

Fujian Provincial Key Laboratory of Quantum Manipulation and New Energy Materials,
College of Physics and Energy, Fujian Normal University,
Fuzhou 350117, P. R. China
**zghuang@fjnu.edu.cn*

Received 26 March 2014
Revised 4 May 2014
Accepted 12 May 2014
Published 27 June 2014

Work functions of Cr/Ni(111), Cr/Ni(100) and Cr/Ni(110) surfaces with different magnetic configurations for Cr atoms in the topmost Cr monolayer are investigated using first-principles methods based on density functional theory. The calculated results reveal that work functions vary with crystal orientations and magnetic configurations. The magnitude of the Cr magnetic moments for the three (111), (100) and (110) surfaces follows a change trend with $M_{\mathrm{Cr,Cr/Ni(111)}} < M_{\mathrm{Cr,Cr/Ni(100)}} < M_{\mathrm{Cr,Cr/Ni(110)}}$. Altering the magnetic configurations of the systems from an original ground state to an excited one will have the total energy and the Fermi level increase. Consequently, it will give rise to the reduction of the work function for the system. Moreover, the quite favorable variation range (4.92–4.41 eV) of the calculated work functions for Cr/Ni(100) system modulated by spin effect implies that the Cr/Ni(100) system may be a more promising candidate. Our work suggests that changing magnetic configurations can modulate the work functions of magnetic metal gates well.

Keywords: First-principles method; work function; magnetic configuration.

PACS numbers: 73.30.+y, 68.35.Dv, 68.35.bs

1. Introduction

Further reduction of semiconductor devices leads to negative effects such as poly-Si depletion, poly-Si dopant penetration and gate leakage. The solution proposed to this problem was the adoption of the gate dielectric with a high dielectric constant to replace traditional SiO_2 and suitable metal gates to replace polycrystalline Si.[1,2] The suitable metal gates need to satisfy the requirement of having two separate work functions which are near the energies of the band edges of Si (about 4.1 eV and 5.1 eV for NMOS and PMOS, respectively).[3,4] However, the selection of suit-

able gate metals is not basically achievable, because usual gate metals are unable to also have two desired work functions. Therefore, substantial effort has been devoted to the tuning of the metal work function to the band edges. These include alloying modulation for binary alloys and bilayer metal gate technology.[5–8] Meanwhile, theoretically, several methods to tune work function have been proposed, such as surface alloy composition, surface orientation,[9,10] and surface adsorption of atom.[11–13] But, even so, the tuning of metal work function is not easily achievable.

The famous discovery of the giant magneto-resistance (GMR) was observed in antiferromagnetic (AFM) coupled layer structures, as a consequence of the fact that the relative orientation of the magnetization of layers changes from antiparallel to parallel in an applied field.[14] In other words, the resistance of the magnetic materials can be modulated by the reorientation of the magnetizations. Furthermore, in the early theoretical studies, Freeman and Alden *et al.* found that spin polarization had a very important role on the work functions of Fe, Co, Ni and Cr,[15–18] for example, the calculated work function (4.05 eV) for Cr(001) with ferromagnetic (FM) state is 0.4 eV lower than that with paramagnetic state.[13] But, it must be specially pointed out that the so-called paramagnetic states in their studies are actually the nonspin polarization states rather than the authentic paramagnetic states. In other words, the variation of the work functions in their studies comes from the difference between FM state and nonspin polarization state. Inspired by the discovery of GMR and the theoretical studies in Refs. 15–18, we have proposed a new method to tune magnetic metal work function via the reorientation of spins for Cr/Fe(001) metal gate.[19] It is found that the spin configuration plays a significant role in determining the work function of the system.

Ni has become a more ideal metal gate material because of its high power function, thermal stability and good compatibility with high-k medium material. However, for Ni-based materials, there objectively exists spin polarization, so in the calculation of work function, the spin polarization should be considered. Moreover, Cr–Cr and Cr–Ni are commonly considered to prefer antiferromagnetic AFM alignment which is similar to Cr–Fe. However, Ni atoms on low index surfaces such as Ni(111), Ni(100) and Ni(110) always prefer FM alignment. Therefore, there may exist comparatively complicated magnetic configurations in Cr/Ni(111), Cr/Ni(100) and Cr/Ni(110) surface systems with one Cr monolayer. In this paper, by means of first principles calculation, the work functions of the Cr/Ni(111), Cr/Ni(100) and Cr/Ni(110) surfaces with various magnetic configurations of Cr atoms were investigated. It is found that work functions of the three surfaces with different magnetic configurations are dependent on different crystal orientations. Altering the magnetic configuration of the system from an original ground state which contains Cr–Cr AFM coupling to an excited one will lead to the increase of the total energy and the Fermi level. As a result, the work function of the system decreases with the increase of the Fermi energy. It is suggested that there exists a promising way to modulate the work function by changing magnetic configurations of the magnetic metal gates. Moreover, the quite favorable variation range (4.92–4.41 eV)

of the calculated work functions for Cr/Ni(100) system modulated by spin effect implies that the Cr/Ni(100) system may be a more promising candidate.

2. Method

The work functions of the Cr/Ni(111), Cr/Ni(100) and Cr/Ni(110) metal surfaces containing one Cr monolayer with different magnetic configurations were calculated by means of first-principles calculation. The calculations were performed using Vienna *ab initio* simulation package (VASP) with projector augmented wave approach[20] The exchange correlation energy was calculated using PW91 generalized gradient approximation.[21] The clean Ni surfaces, Cr/Ni(111), Cr/Ni(100) and Cr/Ni(110) surface models were created by placing a 15 Å vacuum layer on top of a nine-layer slab with a (2×2) unit cell. Monkhorst–Pack k mesh was adopted for all the calculations, a $5 \times 5 \times 1$ k-point mesh for Cr/Ni(111) or Cr/Ni(100) and a $4 \times 5 \times 1$ k mesh for Cr/Ni(110). And the plane-wave basis cutoff energy was 350 eV. Dipole corrections used to handle the asymmetric nature of the two sides of the slabs were considered. Ionic relaxation was performed using the conjugate-gradient Algorithm.[22] After relaxation, the work functions were calculated as the differences between the vacuum level and the Fermi level.[23] By the calculations, the lattice constant for fcc Ni bulk crystal structure was obtained to be 3.513 Å (with a k-point mesh of $11 \times 11 \times 11$), which is slightly less than the experimental value of 3.52 Å. And a 1×1 surface unit cell was used to test the number of layers to ensure the convergence of the work function. The variation for the work function is about 0.01 eV with increasing number of layers. The test results indicated that the convergence needed at least a minimum of four metal layers in a surface model. Therefore, slabs of nine-layer with a 2×2 surface unit cell were chosen in subsequent calculations of work functions for all surfaces. During our calculations, four bottom layers were frozen.

3. Results and Discussion

First, we calculated the work functions for clean Ni(111), Ni(100) and Ni(110) surfaces with FM magnetic configuration. The calculated work functions and magnetic moments of surface Ni atoms (M_{Sur}) for clean Ni surfaces in different crystal orientations are summarized in Table 1. From the table, it is found that the work functions for (111), (100) and (110) surfaces are 5.10, 4.95 and 4.57 eV, respectively, which are dependent on the crystal orientation. The calculated results are consistent with other calculated and experimental results.[24–26] As can also be seen in Table 1, the values of magnetic moments M_{Sur} for three surfaces follow the change trend of $M_{\mathrm{Sur(111)}} < M_{\mathrm{Sur(100)}} < M_{\mathrm{Sur(110)}}$. It is well-recognized that, on a 3d transition metal surface, the magnetic moment enhancement comes from the reduced number of nearest neighbors and weaker interatomic hybridization. For fcc Ni, one atom on (111) crystal surface has six nearest neighbors in the topmost layer and three in the second layer, as seen in Fig. 1(a). One atom on (100) crystal surface has four

Table 1. The calculated work functions, magnetic moments of surface M_{Sur} (μ_B) for clean Ni(111), Ni(100) and Ni(110) surfaces.

		Work function (eV)	
	M_{Sur} (μ_B)	This work	Other calculation and Experiment
Ni(111)	0.67	5.13	5.11[a]
Ni(100)	0.73	4.93	4.97[b]
Ni(110)	0.76	4.57	4.61 ± 0.04[c]

[a]Ref. 24, [b]Ref. 25, [c]Ref. 26.

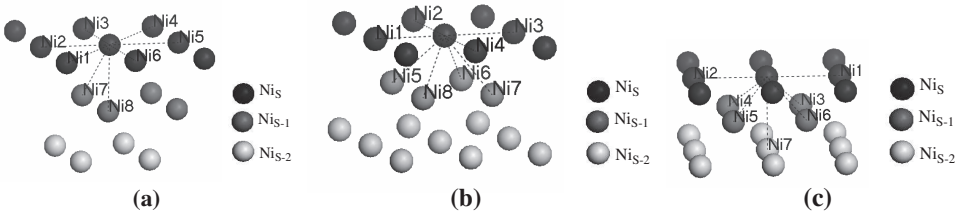

Fig. 1. Distribution of nearest neighbor atoms of one surface atom for (a) Ni(111), (b) Ni(100) and (c) Ni(110).

nearest neighbors in the topmost layer and four in the second layer, as shown in Fig. 1(b). And for (110) crystal surface, as shown in Fig. 1(c), one surface Ni atom only has two nearest neighbors in the topmost layer and four in the second layer and one in the third layer. Thus the number of nearest neighbors of one surface atom for the three surfaces follows the order $N_{\mathrm{Ni(111)}} > N_{\mathrm{Ni(100)}} > N_{\mathrm{Ni(110)}}$, which explains the order of M_{Sur} for the three crystal surfaces well.

During the structural optimization, magnetic moments of Ni substrate atoms were set to be parallel to each other for FM coupling, and the atomic magnetic moments were restricted to collinear orientation. At the same time, different magnetic configurations of Cr atoms in the topmost layer were considered. The magnetic configurations are named as follows that, (1) all Cr atom moments parallelly aligned to each other within Cr layer and antiparallelly aligned to the Ni substrate atom moments is called as APL state; (2) all Cr atom moments parallelly aligned to each other within Cr layer and parallelly aligned to the substrate Ni atom moments is called as PL state; (3) three frustrated collinear configurations within Cr layer are called as mixed (MI) states. The three MI states are considered as follows: MI-1 state: one Cr atom is parallel to Ni moments and other Cr atom moments are antiparallel to Ni moments; MI-2 state: two Cr atom moments are parallel to Ni moments and other Cr atom moments are antiparallel to Ni moments; MI-3 state: three Cr atom moments are parallel to Ni moments and other Cr atom moments are antiparallel to Ni moments. Figures 2(a)–2(e) show five configurations (APL, PL, MI-1, MI-2 and MI-3) for Cr/Ni(111), respectively. Figures 2(f)–2(j) show five configurations for Cr/Ni(100), respectively. Figures 2(k)–2(o) show five configurations

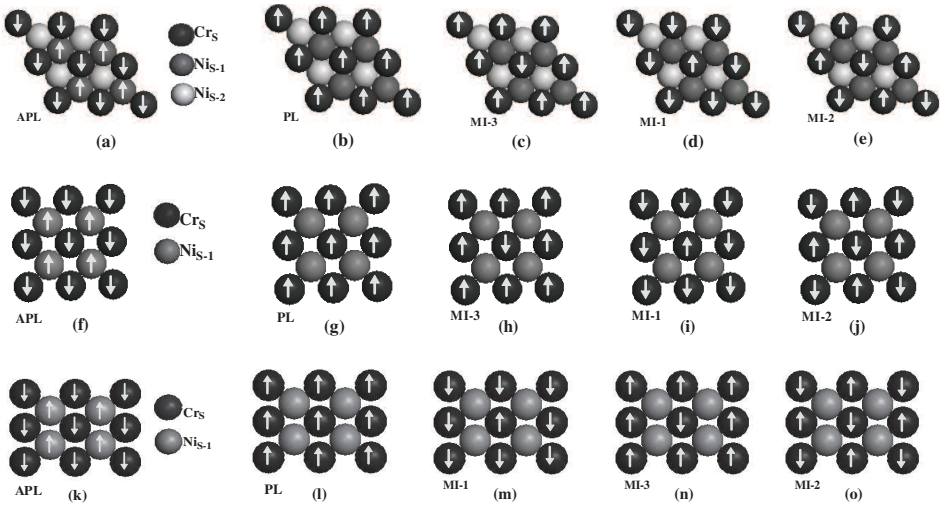

Fig. 2. Various magnetic configurations (a)–(e) for Cr/Ni(111), (f)–(j) for Cr/Ni(100) and (k)–(o) for Cr/Ni(110). The arrow directions indicate the spin-up and spin-down of magnetic moments.

for Cr/Ni(110), respectively. The spin orientations of the substrate Ni atoms are upward, as shown in Figs. 2(a), 2(f) and 2(k), and the spin orientations of Cr atoms in the topmost layer (Cr_S) exhibit different behaviors (be antiparallel or parallel to Ni atoms). In the calculations, energetically, it was found that the optimized structures relaxed with MI-2 state as initial magnetic configuration were always more favorable than that with other states for all three surfaces. Therefore, we used those optimized structures relaxed from MI-2 states to investigate the spin effect of the work functions for three surfaces (Cr/Ni(111), Cr/Ni(100) and Cr/Ni(110)). According to magnetic theory, when a large enough external magnetic field with a specific direction is applied, all spin orientations will rotate to the external field direction. In other words, the magnetic configuration may be changed by applying an external magnetic field. In order to investigate deeply the effect of the spin alignment on the work function, we calculated the work functions of three surfaces with different magnetic configurations by constraining the direction of magnetic moment.

Figures 3(a) and 3(b) show the calculated work functions Φ(eV) and the Fermi energies E_F(eV) of the three surface structures with various corresponding magnetic configurations in Fig. 2, respectively. From the figures, one can see clearly that for the given surface (such as Cr/Ni (111)), the lower the Fermi energy E_F is, the larger the work function of the system is. And the dependence of work function on crystal orientation is similar to the case of the three clean Ni surfaces. That is, the work function for (111) surface is largest, while one for (110) is least. From Fig. 3(a), we can find that the work functions of all three surfaces vary with magnetic configurations. Especially, for Cr/Ni(111) and Cr/Ni(100) surfaces, the variety is more obvious. For Cr/Ni(111), the maximal changed value of work functions reaches

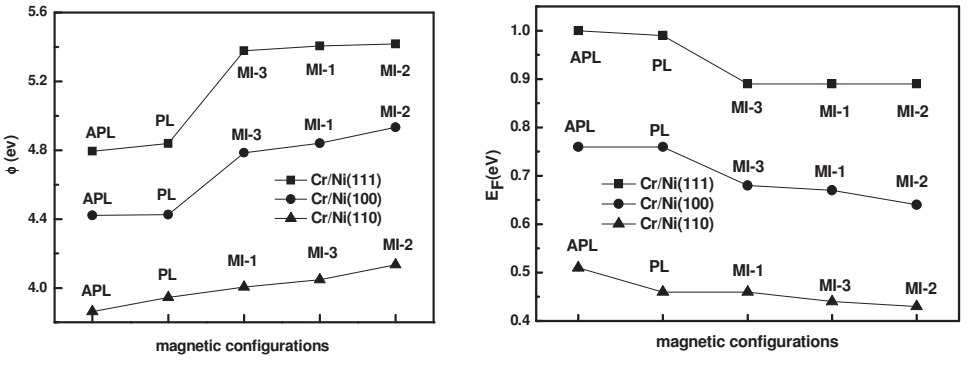

(a) (b)

Fig. 3. Work functions Φ (a) and Fermi energies E_F (b) for Cr/Ni(111), Cr/Ni(100) and Cr/Ni(110) surfaces with the corresponding different magnetic configurations presented in Fig. 2.

about 0.63 eV. For Cr/Ni(100), the general changed trend of the work functions is similar to that for Cr/Ni(111), but the maximal changed value of work functions (about 0.51 eV) is slightly smaller than that for Cr/Ni(111). For Cr/Ni(110), the changed value of the work functions is little. These differences should be attributed to the different surface structures of different crystal surfaces. Being similar to the three foregoing clean Ni surfaces, one surface Cr atom on Cr/Ni(111) surface has six nearest neighbor Cr atoms in the topmost layer and three nearest neighbor Ni atoms in the second layer. One surface Cr atom on Cr/Ni(100) surface only has four nearest neighbor Cr atoms in the topmost layer and four nearest neighbor Ni atoms in the second layer. And one surface Cr atom on Cr/Ni(110) only has two nearest neighbor Cr atoms in the topmost layer and four nearest neighbor Ni atoms in the second layer and one nearest neighbor Ni atom in the third layer. Hence, for the three surfaces, the number of the nearest neighbor Cr–Cr and Cr–Ni bonds follows $N_{\mathrm{Cr/Ni(111)}} > N_{\mathrm{Cr/Ni(100)}} > N_{\mathrm{Cr/Ni(110)}}$. Of course, the effects of spin alignment on the work function become less with the decrease of the number of the nearest neighbor Cr–Cr and Cr–Ni bonds. This is a possible reason to explain the changed trend of work function from Cr/Ni (111) to Cr/Ni (100) and to Cr/Ni (110), shown in Fig. 3(a). Moreover, it can be seen from Fig. 3(a), for Cr/Ni(111), the tuning range for work function between MI-2 state and PL state reaches about 0.58 eV (5.42 eV for MI-2 state, 4.84 eV for PL state). And for Cr/Ni(100), it reaches about 0.51 eV (4.92 eV for MI-2 state, 4.41 eV for PL state). These results indicate that changing magnetic configurations of the system should be a promising way to modulate the work function. Moreover, from the view of the tuning ranges of the work function, the Cr/Ni(100) system may be a more ideal metal gate for spin modulation. Because its two work functions for MI-2 state ($\Phi = 4.92$ eV) and PL state ($\Phi = 4.41$ eV) are close to Si band edges for PMOS and NMOS, respectively and altering the MI-2 ground state to PL excited state is easy to achieve by applying a magnetic field paralleling to magnetic moment of substrate atoms.

Table 2. The calculated work functions, Φ(eV), total energy, E(eV) and calculated magnetic moments (μ_B) of the topmost three layer atoms, for Cr/Ni(111) with various magnetic configurations shown in Figs. 2(a)–2(e).

		Different magnetic configurations				
		APL	PL	MI-3	MI-1	MI-2
Magnetic moment (μ_B)	$Cr_{(S)}$	−1.328, −1.310 −1.420, −1.420	1.330, 1.312 1.422, 1.422	1.361, 1.3435 −1.452, −1.514	−1.361, −1.343 −1.453, −1.513	1.417, 1.399 −1.506, −1.516
	$Ni_{(S-1)}$	0.076, 0.076 0.148, 0.153	0.055, 0.055 0.127, 0.132	0.061, 0.128 0.061, 0.128	0.068, 0.146 0.068, 0.146	0.071, 0.144 0.071, 0.144
	$Ni_{(S-2)}$	0.598, 0.598 0.580, 0.580	0.596, 0.596 0.577, 0.577	0.595, 0.576 0.595, 0.576	0.598, 0.579 0.598, 0.579	0.603, 0.578 0.603, 0.578
Φ(eV)		4.79	4.84	5.38	5.41	5.42
E(eV)		1.62	1.70	0.51	0.44	0.00

Table 3. The calculated work functions, Φ(eV), total energy, E(eV) and calculated magnetic moments (μ_B) of the topmost three layer atoms, for Cr/Ni(100) with various magnetic configurations shown in Figs. 2(f)–2(j).

		Different magnetic configurations				
		APL	PL	MI-3	MI-1	MI-2
Magnetic moment (μ_B)	$Cr_{(S)}$	−2.387	2.391	2.384, 2.431 2.431, −2.474	2.473, −2.432 −2.432, −2.383	2.504, −2.464 2.505, −2.464
	$Ni_{(S-1)}$	0.314	0.289	0.296	0.308	0.300, 0.294 0.300, 0.294
	$Ni_{(S-2)}$	0.587, 0.577 0.587, 0.577	0.577, 0.587 0.577, 0.587	0.586, 0.579 0.586, 0.579	0.579, 0.587 0.579, 0.587	0.589, 0.569 0.589, 0.569
Φ(eV)		4.41	4.41	4.79	4.86	4.92
E(eV)		3.73	3.48	1.34	1.50	0.00

Table 2 lists the calculated total energies E, work functions Φ and magnetic moments of the topmost three layer atoms ($Cr_{(S)}$, $Ni_{(S-1)}$, $Ni_{(S-2)}$) for Cr/Ni(111) surface with APL, PL and three MI states. Similarly, Table 3 is for Cr/Ni(100) surface, and Table 4 for Cr/Ni(110) surface. From Tables 2–4, one can notice that: (1) From a view of the total energy, for all three surfaces, the MI-2 states prefer to be ground states. And generally, various MI states are more stable than the APL and PL states. It is suggested that the AFM coupling among Cr atoms on surface layer is intrinsic. Nevertheless, if the stable magnetic configurations of the system contain Cr–Cr AFM coupling, then it is possible for one to alter the magnetic configuration by applying an external magnetic field. For example, when a large enough upward external magnetic field is applied, the systems which are originally

Table 4. The calculated work functions, Φ(eV), total energy, E(eV) and calculated magnetic moments (μ_B) of the topmost three layer atoms, for Cr/Ni(110) with various magnetic configurations shown in Figs. 2(k)–2(o).

		Different magnetic configurations				
		APL	PL	MI-3	MI-1	MI-2
Magnetic moment (μ_B)	$Cr_{(S)}$	−2.974, −2.926 −2.974, −2.926	2.979, 2.930 2.979, 2.930	3.029, −2.975 −2.975, −2.926	2.979, 2.930 3.028, −2.977	2.984, −2.927 2.984, −2.928
	$Ni_{(S-1)}$	0.231	0.206	0.226	0.214	0.226
	$Ni_{(S-2)}$	0.420, 0.474 0.420, 0474	0.415, 0.470 0.415, 0.470	0.470, 0.426 0.470, 0.426	0.415, 0.476 0.464, 0.422	0.475, 0.417 0.475, 0.417
Φ(eV)		3.86	3.94	4.00	4.05	4.13
E(eV)		2.19	1.85	0.99	0.80	0.00

at the MI-2 ground states [see Figs. 2(e), 2(j) and 2(o)] will turn into the PL excited states [see Figs. 2(b), 2(g) and 2(i)]. That is, the magnetic moments of Cr atoms with down orientation in the ground state flip their directions to be parallel to the applied magnetic field. This causes the increase of the total energy and the lifting of the Fermi level, which gives rise to the decrease of the work function. (2) There exists a huge moment enhancement for the Cr monolayer on all the three Ni surfaces compared to the Cr bulk moment. Moreover, as can also be seen in Tables 2–4, the magnetic moments of Cr atoms (M_{Cr}) for three surfaces follow the trend of $M_{Cr,Cr/Ni(111)} < M_{Cr,Cr/Ni(100)} < M_{Cr,Cr/Ni(110)}$. This can be explained as the same as the change of M_{Sur} for the three clean Ni surfaces. There are six Cr nearest neighbors and three Ni nearest neighbors for Cr/Ni(111), four Cr and four Ni for Cr/Ni(100), two Cr and five Ni for Cr/Ni(110). The smaller the number of nearest neighbors is, the larger the enhancement of M_{Cr} is. Furthermore, Cr–Ni interatomic coupling is weaker than Cr–Cr interatomic coupling, so the larger the proportion of Cr–Ni nearest neighbors in the total Cr–Cr and Cr–Ni nearest neighbors, the larger the enhancement of M_{Cr} is. Consequently, the corresponding M_{Cr} presents the following trend: $M_{Cr,Cr/Ni(111)} < M_{Cr,Cr/Ni(100)} < M_{Cr,Cr/Ni(110)}$. (3) The magnetic moments of the second and third layer Ni atoms ($M_{Ni(S-1)}$ and $M_{Ni(S-2)}$) are decreased compared to its bulk moment. $M_{Ni(S-1)}$ and $M_{Ni(S-2)}$ are influenced by the mutual interaction of the substrate Ni atoms and the surface Cr atoms. The mutual interaction gives rise to a decreased magnetic moment of $Ni_{(S-1)}$ and $Ni_{(S-2)}$. These decreases of $M_{Ni(S-1)}$ and $M_{Ni(S-2)}$ are similar to the results for the interface magnetism of Cr/Ni with fcc crystal structure in Ref. 27. Moreover, the moments of Ni atoms in the more inner layers are hardly influenced by the surface Cr atoms. Thus the magnetic moments of $Ni_{(S-2)}$ are close to that of bulk. This tendency can also be seen from the density of states in Fig. 4. Figure 4 shows the spin-resolved LDOS of Cr atom in the first topmost layer, Ni atoms in the topmost

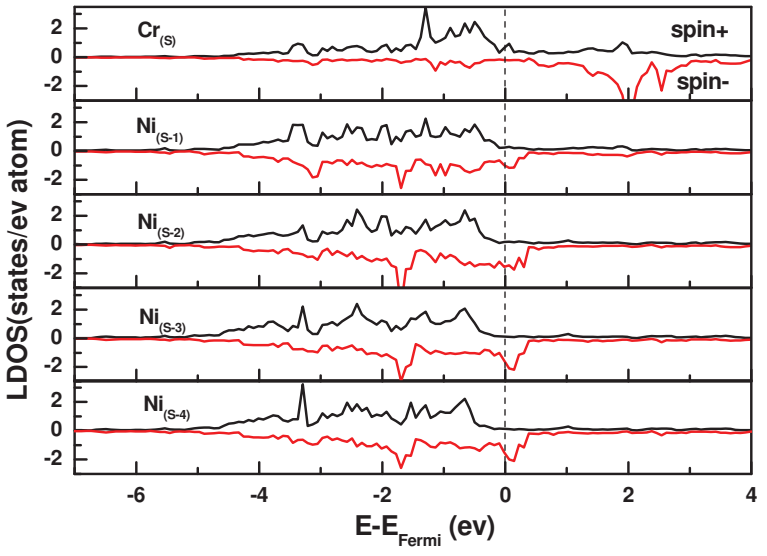

Fig. 4. Local density of states (LDOS) for the surface $Cr_{(S)}$ atom and substrate atoms $Ni_{(S-1)}$–$Ni_{(S-4)}$ atoms of Cr/Ni(100) surface with MI-2 state.

four layers ($Ni_{(S-1)}Ni_{(S-4)}$) near the Cr surface layer for Cr/Ni(100) surface with MI-2 state. From the figure, it is also clearly seen that $Ni_{(S-2)}$ atoms are slightly affected by Cr atoms, and its LDOS is close to that of $Ni_{(S-3)}$ and $Ni_{(S-4)}$ atoms. It is in agreement with the smaller change of the magnetic moment of $Ni_{(S-2)}$ atoms. On the contrary, the LDOS of Cr atom in the topmost layer and Ni atom in the second layer have the bigger changes in the region near Fermi energy. This may be contributed mainly by the *d*–*d* hybridization between the surface Cr atom 3d state and the Ni substrate 3d state. Similarly, the variations of the LDOS of Cr atom and Ni atoms for Cr/Ni(111) and Cr/Ni(110) surfaces are similar to the case of Cr/Ni(100). (4) The layer dependence of the calculated magnetic moments in Tables 2–4 is similar to that for the Mn monolayer on Ni(001), Ni(011) and Ni(111) in Ref. 28. It is found that there is one value or two values for the Cr moment, which is similar to that there exists one value or two values for the Mn moment. Moreover, for (001) and (011), it is observed that there is only single Ni moment for S-1 Ni layer from the data in Tables 3 and 4, which is consistent to single Ni moment with $M(\mathrm{Ni_{Ja}}) = M(\mathrm{Ni_{Jb}})$ for S-1 Ni layer of Mn/Ni.

When the external field is large enough, the number of up spins and down spins could occur to reverse relative to the original ground state. Thus the direction of the net magnetic moment should reverse to that of the applied field. As a result, the magnetic configuration of the system can be changed. As an example, for Cr/Ni(100) surface, the magnetic configuration turns from MI-2 ground state to PL excited state. The inversion of Cr magnetic moment can be clearly seen from the change of the spin-polarized LDOS shown in Fig. 5. As shown in Fig. 5, the

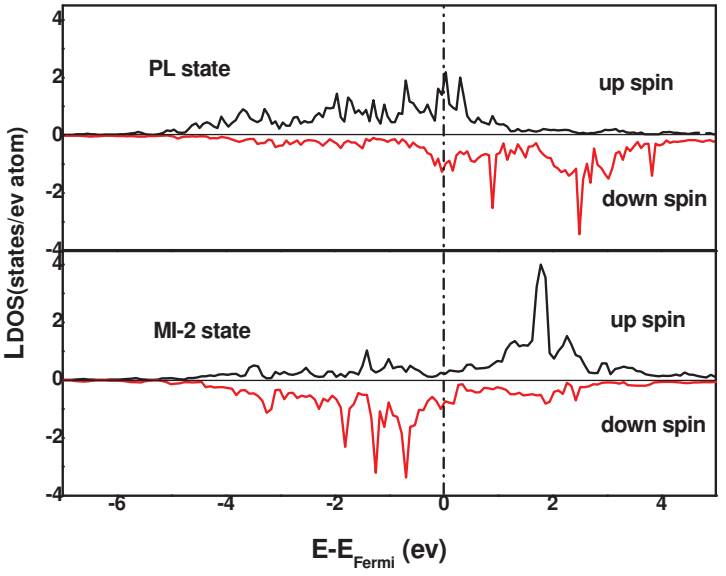

Fig. 5. LDOS for the surface Cr atom of Cr/Ni(100) with MI-2 and PL states.

DOS of up spins with PL excited state near Fermi level increases and that of down spins decreases inversely relative to the DOS of spins with MI-2 ground state. The behavior of the DOS is coincident with the change of Cr magnetic moments listed in Table 3.

4. Conclusion

We have investigated the work functions of the Cr/Ni(111), Cr/Ni(100) and Cr/Ni(110) surfaces with different magnetic configurations. The calculated results indicate that the work functions of three surfaces vary with various magnetic configurations. The changes of the work function for Cr/Ni(111) and Cr/Ni(100) surfaces are more obvious than that for Cr/Ni(110) surface. The maximal change value of work functions reaches about 0.63 eV for Cr/Ni(111); a slightly smaller change value is about 0.51 eV for Cr/Ni(100); a least change value is about 0.27 eV for Cr/Ni(110). A huge moment enhancement for Cr monolayer on three Ni surfaces compared to the Cr bulk moment is found, and the magnetic moments of Cr atoms for three surfaces follow the trend of $M_{\mathrm{Cr,Cr/Ni(111)}} < M_{\mathrm{Cr,Cr/Ni(100)}} < M_{\mathrm{Cr,Cr/Ni(110)}}$, which is due to their different surface structures. The results also reveal that, when the magnetic configuration of the system is changed from the ground state into an excited one, the total energy is increased and the Fermi level is enhanced. As a result, the work function of the system is decreased. It is considered that changing magnetic configurations of the system is a possible way to tune the work functions. Especially, the variation range of the calculated work function for Cr/Ni(100) system from MI-2 state ($\Phi = 4.92$ eV) to PL state ($\Phi = 4.41$ eV)

is near 5.1–4.1 eV, thus it may be a promising candidate for spin-modulated work function.

Acknowledgments

This work is supported by the National Science Foundation of China (11004039, 11204038), National Key Project for Basic Research of China under Grant No. 2011CBA00200, Educational Department of Fujian Province, China (JA11058).

References

1. G. D. Wilk, R. M. Wallace and J. M. Anthony, *J. Appl. Phys.* **89**, 5243 (2001).
2. E. P. Gusev, V. Narayanan and M. M. Frank, *IBM J. Res. Dev.* **50**, 387 (2006).
3. I. De *et al.*, *Solid-State Electron.* **44**, 1077 (2000).
4. Y. F. Dong *et al.*, *Phys. Rev. B* **73**, 045302 (2006).
5. A. V. Zenkevich *et al.*, *J. Appl. Phys.* **111**, 07C506 (2012).
6. M. Chang *et al.*, *J. Appl. Phys.* **113**, 034107 (2013).
7. R. P. Birringer *et al.*, *J. Appl. Phys.* **108**, 053704 (2010).
8. C. L. Hinkle *et al.*, *Appl. Phys. Lett.* **100**, 153501 (2012).
9. G. Xu *et al.*, *Phys. Rev. B* **78**, 115420 (2008).
10. G. Xu *et al.*, *J. Appl. Phys.* **106**, 043708 (2009).
11. D. F. Li *et al.*, *Physica B* **392**, 217 (2007).
12. S. Yamagishi, S. J. Jenkins and D. A. King, *Surf. Sci.* **12**, 543 (2003).
13. G. Xu *et al.*, *Acta. Phys. Sin.* **58**, 1924 (2009).
14. M. N. Baibich *et al.*, *Phys. Rev. Lett.* **61**, 2472 (1988).
15. C. L. Fu and A. J. Freeman, *Phys. Rev. B* **33**, 1755 (1986).
16. R. Wu and A. J. Freeman, *Phys. Rev. B* **47**, 3903 (1993).
17. M. Alden *et al.*, *Phys. Rev. B* **46**, 6303 (1992).
18. O. Rader and W. Gudat, *Phys. Rev. B* **55**, 5404 (1997).
19. K. Zhong *et al.*, *AIP Adv.* **2**, 042134 (2012).
20. G. Kresse and J. Joubert, *Phys. Rev. B* **59**, 1758 (1999).
21. J. P. Perdew, K. Burke and M. Ernzerhof, *Phys. Rev. Lett.* **77**, 3865 (1996).
22. W. H. Press *et al.*, *New Numerical Recipes* (Cambridge University Press, New York, 1986).
23. N. D. Lang and W. Kohn, *Phys. Rev. B* **3**, 1215 (1971).
24. F. Mittendorfer, A. Eichler and J. Hafner, *Surf. Sci.* **423**, 1 (1999).
25. B. Xing *et al.*, *J. Mol. Catal. A*: *Chem.* **187**, 315 (2010).
26. M. Busch, S. Wethekam and H. Winter, *Nucl. Instrum. Methods. Phys. Res. B* **267**, 2625 (2009).
27. A. M. N. Niklasson, B. Johansson and H. L. Skriver, *Phys. Rev. B* **59**, 6373 (1999).
28. B. R. Malonda-Boungou *et al.*, *Phy. Rev. B* **81**, 024402 (2010).